Heat conduction in a solid substrate with a spatially-variable solar radiation input: Carslaw-Jaeger solution revisited

R.G. Kasimova[1], Yu.V.Obnosov[2]

[1]German University of Technology in Oman, Muscat, Sultanate of Oman

[2]Institute of Mathematics and Mechanics, Kazan Federal University, Kazan, Russia

Abstract
Temperature distributions recorded by thermocouples in a solid body (slab) subject to surface heating are used in a mathematical model of 2-D heat conduction. The corresponding Dirichlet problem for a holomorphic function (complex potential), involving temperature and heat stream function, is solved in a strip. The Zhukovskii function is reconstructed through singular integrals, involving an auxiliary complex variable. The complex potential is mapped by the Schwartz-Christoffel formula onto an auxiliary half-plane. The final heat conduction flow net (orthogonal isotherms and heat lines) is compared with the known Carslaw-Jaeger solution and shows a puzzling topology of energy fluxes for simple temperature-boundary conditions.
Key words: Laplace's equation, topology of heat lines, complex potential, conformal mappings.

1. Introduction

Analytical solutions to potential field problems, where the intricate topology of 2-D flow nets (stream lines and constant potential lines) was controlled by heterogeneity of the flow domain, but the boundary conditions were uniform (constant potentials on the inlet and outlet of a standard flow tube) were presented in [1], [2]. In this paper we study the effect of non-uniform boundary conditions, although assume that the medium, through which flow takes place, is homogeneous. Analytical solutions for steady 2-D heat conduction in solid bodies are needed in different engineering designs involving heat transfer [3]. A powerful technique to solve these problems is based on the theory of boundary-value problems for holomorphic functions (e.g., [4], [5]). In this paper we average the diurnal temperature swings, recorded by thermocouples on the surface of a concrete slab, and show that the corresponding explicit analytical solution gives a computer-algebra-visualized topology of heat lines, which is counterintuitive and puzzling.

2. Mathematical Model

We consider a vertical cross-section of the slab of a thickness b and thermal conductivity k, and a thermal barrier E_1OE_2 (practically, strip-type shading against solar radiation). Fig.1a depicts a vertical cross-section and Cartesian coordinates. Far from the barrier (the rays AE_1 and E_2B), the slab temperature is the same as the ambient air temperature, T_0 =constant. Along AOB, we have experimental data of temperature obtained by thermocouples and we take the daily averages of these values. The x-distribution of this average temperature is a single-minimum function f(x). We assume that this function is symmetric f(-x)=f(x) and $f(x) \to T_0$ at $x \to \pm\infty$ (this is confirmed by experiments). We introduce F(x) as:

$$f(x)=T_0 - F(x), \quad \text{at } y=0 \qquad (1)$$

where F(x) is a single-maximum ($T_M = T_0 - T_m$) function shown in Fig.1b. We assume that along the internal surface (DC in Fig.1a) temperature is constant, T_c:
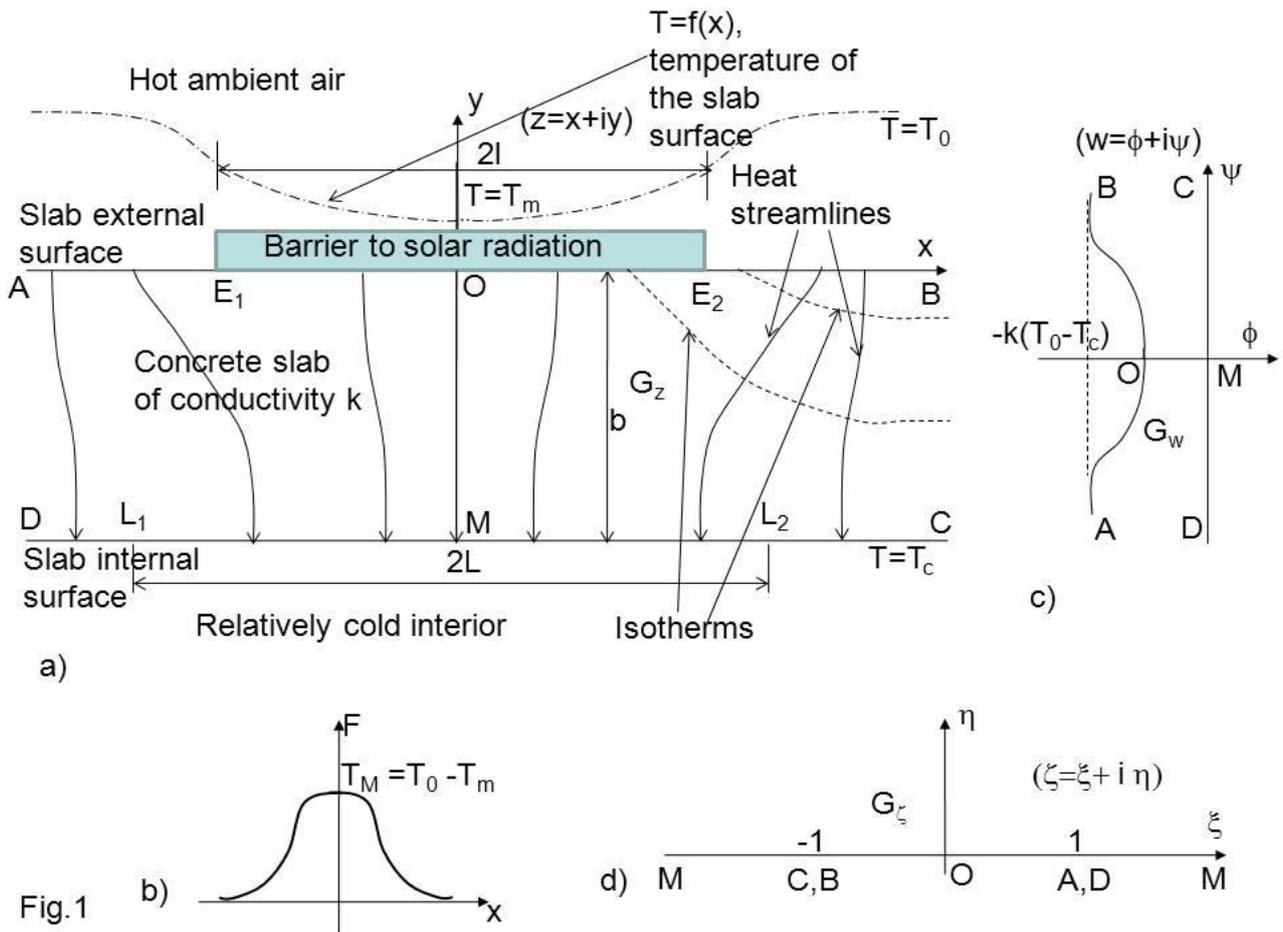
$$T=T_c, \quad \text{at } y=-b \qquad (2)$$

Fig.1. Vertical cross-section of a slab with a thermal barrier (a), temperature boundary condition on the exterior surface – the kernel of the Cauchy integral (b), complex potential domain for small T_M (c), auxiliary plain where the Dirichlet problem is solved (d).

Fig.2. Heat line topology with four hinge points (a), the corresponding knob-shape bounded complex potential domain (b).
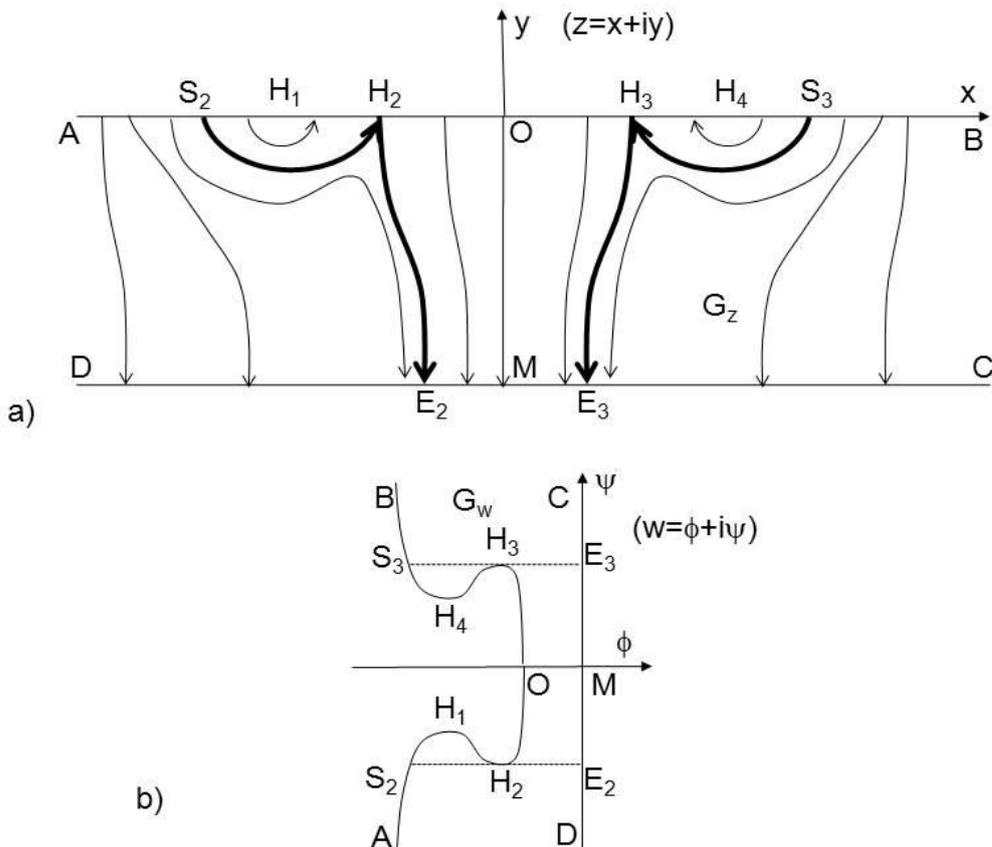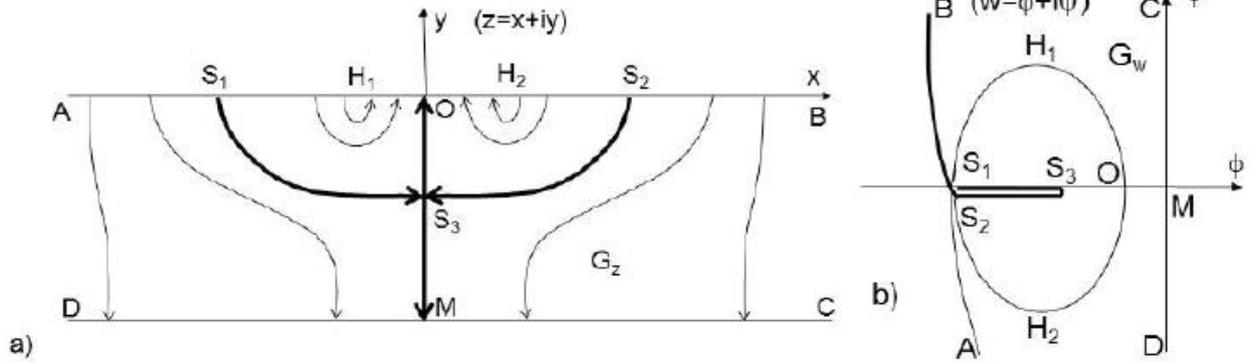
In case of no thermal barrier in Fig.1a, heat conduction in the slab of Fig.1a is 1-D. With the barrier, the so-called "thermal resistor" models (see, e.g., [6]) have been used. The resistor approximation assumes the AOB boundary condition to be a step-function (reflecting the barrier width) and the heat streamlines are postulated to be straight and perpendicular to the both slab boundaries, i.e. heat flow is again 1-D. Our objective is to assess analytically the spatial nonuniformity of temperature and heat lines caused by the boundary condition (1).

According to the Fourier law, heat conduction in the strip AOBCMD (we denote it G_z) of Fig.1a is governed by

$$\vec{J} = -k\nabla T(x, y) \qquad (3)$$

where $\vec{J}(x, y)$ is the heat flux vector, which has a

spherical, etc. coordinate system, where the Laplace equation separates). Our method does not have this limitation and is applicable to any G_z-polygon with arbitrary mixed (Dirichlet-Newman) boundary.

Without any loss of generality we assume that along OM $\psi=0$ that follows from the symmetry of f(x). The isotherms (equipotential lines ϕ=const) are dashed in Fig.1a and heat streamlines (ψ =const) are shown in bold with arrows indicating the direction of heat transfer. The domain G_z is fixed but the domain corresponding to G_z in the w-plane, G_w, depends on f(x) and is surprisingly complex even for simple functions f(x).

If T_m is close to T_0 and the slope of f(x) is small, then G_w is a strip with a slightly bulged side AOB (Fig.1c). The streamlines in G_z (Fig.1a) are somewhat curved, most of all in the slab zones where the imposed f(x) has a relatively high slope magnitude |df/dx| (see Fig.1a).

a)

b)

Fig.3. Heat line topology with two hinge points (a), the corresponding double-sheet Riemann surface as the complex potential domain (b).

vertical component v and horizontal component u.

We introduce a complex physical coordinate z=x+iy and a complex potential w=ϕ +i ψ where i is an imaginary unit, ϕ=-k(T-T_c) is the potential and ψ is a stream function, which is related to ϕ through the Cauchy-Riemann conditions:

$$\frac{\partial\phi}{\partial x} = \frac{\partial\psi}{\partial y} = u, \qquad \frac{\partial\phi}{\partial y} = -\frac{\partial\psi}{\partial x} = v \qquad (4)$$

Heat lines ψ=const allow a better visualization of heat transfer and an assessment of thermophysical efficiency [7].

Both ϕ and ψ are harmonic:

$$\Delta\phi(x, y) = 0, \qquad \Delta\psi(x, y) = 0 \qquad (5)$$

and w(z) is a holomorphic function.

An integral solution of the boundary-value problem (1),(2) and (5) is given in [3] (Chapter V, Section 3, eqn.2.19). Here we derive an alternative solution. Carslaw and Jaeger derived their solution by the Fourier transform method. The Laplace equation was analytically solved in [8] in a stream tube G_z by separation of variables and Fourier's series expansions. The Fourier methods are limited to the domains G_z that are homeomorphic to a simple streamtube (two constant temperature - two adiabatic segments as boundaries coinciding with the level lines of a Cartesian, cylindrical,

For a smaller T_m (fixed T_0 but higher T_M) and/or stronger variation of the slope of f(x), the heat flow topology is shown in Fig.2a. On AOB (we recall, f(x) is a single-minimum function) at four points H_1, H_2, H_3, and H_4, the direction of the v-component of the thermal gradient changes from inside the slab to the exterior. Indeed, along AS_2H_1 and BS_3H_4 heat is conducted from the exterior surface into the slab. Along H_1H_2 and H_4H_3 heat is discharged back and along H_2H_3 heat moves from the exterior surface to the interior. There are two separatrices (dividing streamlines shown in bold), $S_2H_2E_2$ and $S_3H_3E_3$, which demarcate five different topological zones in G_z. The corresponding domain G_w is shown in Fig.2b where the image of AOB is a knob-shaped curve.

For even smaller T_m and/or stronger slopes of f(x) we may arrive at topology depicted in Fig.3a. Here we have two points H_1 and H_2 where flow changes its orientation from the interior to the exterior of the slab. The only separatrix (bold-styled in Fig.3a) has a saddle point S_3. Above $S_1S_3S_2$ heat is circulated from the air

into concrete and back, without entering the interior. The domain G_w shown in Fig.3b is a double-sheet Riemann surface. The second sheet $S_1H_1OH_2S_2$ is stitched to the first (main) sheet through the cut $S_1S_3S_2$, which images the separatrix in G_z. In Fig.3b we purposely distorted the branch AS_1 (of course, this branch in G_w is symmetrical to S_2B with respect to the ϕ axes) in order to illustrate the stitching of the second sheet. Points S_1 and S_2 are located on the opposite sides of the cut in G_w. If $T_m < T_c < T_0$, then still another heat conduction regime is realized, with heat flux from the interior (this regime may occur in cold countries and has not been experimentally observed in Oman).

We implement a mathematical technique, which can readily tackle any heat flow regime in Figs.1a-3a. The method is based on a conformal mapping of one domain (G_z in our case) onto an auxiliary domain (circle, half-plane) and, next, solving there a Dirichlet, mixed, Newton (Robin) or refraction problem (with the first to fourth boundary conditions, correspondingly) and further reconstruction of the second holomorphic function in the auxiliary domain ([1], [2]).

So, first, we map conformally G_z onto the upper half-plane Im $\zeta > 0$ of an auxiliary plane $\zeta = \xi + i\eta$ shown in Fig.1d by the Schwartz-Christoffel formula:

$$z = -\frac{b}{\pi}\log\frac{1+\varsigma}{1-\varsigma} \qquad (6)$$

In this plane points A and D, as well as C and B coincide.

Next, we introduce the Zhukovskii function (see [5]) as $Zh = w - i(T_0 - T_c)kz/b + k(T_0 - T_c) = R + i\ I$. The real part of this function is $R = Re[Zh] = \phi + k(T_0 - T_c)y/b + k(T_0 - T_c)$ and the imaginary part is $I = Im[Zh] = \psi - k(T_0 - T_c)x/b$. Obviously, $Zh(z)$ is also holomorphic. In the half-plane Im $\zeta > 0$ the following boundary conditions hold for $Zh(\zeta)$:

$$R = 0 \text{ at } |\xi| > 1, \quad R = kF[x(\xi)] \text{ at } |\xi| < 1 \qquad (7)$$

where eqn.(6) gives $x(\xi)$ as :

$$x = -\frac{b}{\pi}\log\frac{1+\xi}{1-\xi}, \qquad |\xi| < 1,$$

$$x = -\frac{b}{\pi}\log\frac{\xi+1}{\xi-1}, \qquad \xi > 1 \qquad (8)$$

Obviously (see Fig.1b), $F(\xi) \to 0$ at $\xi \to \pm 1.$ The function $F(\xi)$ can be easily interpolated from experimental (thermocouple) daily-averaged point-wise collected values. We used $F[x] = T_M \exp[-ax^2]$, where a is a fitting parameter, as an approximation for experimentally-measured temperature values. Any other function, e.g., $F[x] = T_M /[1+(b_c x)^2]$ (where b_c is another fitting parameter), can be used in eqn.(7) as a boundary condition. Eqn.(8), obtained from the conformal mapping, is fixed and does not depend on interpolation of experimental data and the choice of F[x].

Along with the boundary conditions (7) for the real part of the Zhukovskii function $R(\zeta)$, we note that at point M (where $\zeta \to \infty$) the imaginary part of this complex function, $I(\zeta)=0$. Then an integral solution to the stated Dirichlet boundary-value problem is (see [5]):

$$Zh(\zeta) = -\frac{i}{\pi}\int_{-1}^{1}\frac{kF(\tau)d\tau}{\tau - \zeta} \qquad (9)$$

Passing to the Sokhotsky-Plemelj limit $\zeta \to \xi, \quad |\xi| < 1$ from eqn.(9) we obtain the stream function along AOB:

$$\psi = \frac{k(T_0 - T_c)}{b}x(\xi) - \frac{1}{\pi}\int_{-1}^{1}\frac{kF(\tau)d\tau}{\tau - \xi} \qquad (10)$$

We note that the integral in eqn.(10) is singular at $|\xi| < 1$ (that corresponds to the line AOB in Fig.1a) and should be calculated in the sense of *v.p.* (principal value). Wolfram's *Mathematica* [9] has a routine *CauchyPrincipalValue* for this purpose, which we used in numerical integration. At $|\xi| > 1$ (line DMC in Fig.1a) the integral in eqn.(10) is regular and we used the routine *NIntegrate* from [9].

It is convenient to expand the kernel in eqn.(10) in a series of Chebyshev's polynomials of the second kind as:

$$F(\tau) = T_M\sum_{n=1}^{\infty}b_n U_n(\tau), \quad |\tau| < 1, \quad b_n = \frac{2}{\pi}\int_{-1}^{1}\frac{f(\tau)U_n(\tau)}{\sqrt{1-\tau^2}}d\tau$$

where $U_n(\tau) = \sin[\ n\arccos\tau]$. For any smooth (e.g., belonging to the Holder class is sufficient) function $F(\tau)$ this series is uniformly converging on the interval $(-1,1)$. Then for the roof surface AB eqn. (10) is reduced to

$$\psi = \frac{k(T_0 - T_c)}{b}x(\xi) - k$$

$$T_M\sum_{n=1}^{\infty}b_n T_n(\xi), \qquad |\xi| < 1 \qquad (11)$$

and for the ray MD we have

$$\psi = \frac{k(T_0 - T_c)}{b}x(\xi) + kT_M$$

$$\sum_{n=1}^{\infty}b_n(\xi - \sqrt{\xi^2 - 1})^n, \qquad \xi > 1 \qquad (12)$$

where $T_n(\tau) = \cos[n\arccos\tau]$ are the Chebyshev polynomials of the first kind. For the ray MC ($\xi < -1$) we have $\psi(-\xi) = \psi(\xi)$, i.e. eqn.(12) can be used.

The vertical component of the thermal gradient `

$$v = -\frac{\partial\psi}{\partial x} = -\frac{\partial\psi}{\partial\xi}\left(\frac{\partial x}{\partial\xi}\right)^{-1} \qquad (13)$$

Far from the insulation zone (large values of |x|) the horizontal component u of the gradient vanishes and $v \to v_\infty = -\dfrac{k(T_0 - T_c)}{b}$. We introduce a dimensionless vertical component $v^d = v/v_\infty$. On AOB, differentiation of eqns. (8) and (11) yields

$$v^d(\xi) = 1 - \frac{\pi r}{2}\sqrt{1-\xi^2}\sum_{n=1}^{\infty} nb_n U_n(\xi), \quad |\xi| < 1, \quad r = \frac{T_M}{T_0 - T_c} \quad (14)$$

Then the hinge points (if they exist) in Figs.2a-3a are found from eqn.(14) as the roots of the equation $v^d(\xi) = 0, \quad |\xi| < 1$. We solved this equation using the *FindRoot* routine [9].

How much in terms of total energy saving we gain from thermal insulation? In order to answer this question we select two symmetrical points L_1 and L_2 on the interior surface, distance 2L apart. Without the barrier in Fig.1a, the total heat entering the interior (per unit length in the direction perpendicular to the plane in Fig.1a) through a strip of a width 2L is $Q_0 = 2L\, k(T_0 - T_c)/b$. From the definition of the stream function the total heat flowing through the same area but in 2-D conduction with insulation is $Q = -2\psi_{L1}$, where ψ_{L1} is directly expressed from eqns.(8) and (12) as:

$$\psi_{L1} = \frac{k(T_c - T_0)L}{b} + kT_M \sum_{n=1}^{\infty} b_n \tanh^n\left(\frac{\pi L}{4b}\right) \quad (15)$$

We introduce a dimensionless energy saving through $L_1 L_2$ as $S(L) = \delta Q/Q_0$, where $\delta Q = Q_0 + 2a\psi_{L1}$ and, with ψ_{L1} taken from eqn.(15), we have:

$$\delta Q = r\frac{b}{L}\sum_{n=1}^{\infty} b_n \tanh^n\left(\frac{\pi L}{4b}\right) \quad (16)$$
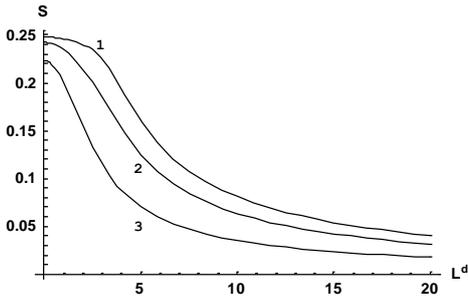

Fig.4. Energy saving factor S as a function of L^d for r=0.25 and a^d=0.025, 0.1 and 0.4 (curves 1-3, correspondingly).

As we have pointed out, the selected F(x) is $T_M \exp[-a x^2]$. Fig.4 shows S as a function of a dimensionless width $L^d = L/b$ for r=0.25 and a^d=0.025, 0.1 and 0.4 (curves 1-3, correspondingly, where $a^d = a\, b^2$), calculated by eqn.(16). In Fig.5 v^d is shown as a function of dimensionless abscissa $x^d = x/b$ along AOD for r=0.5 and a^d=1, 2 and 4 (curves 1-3, correspondingly), calculated by eqn.(14). As

we can see from Fig.5, for the selected F(x) we have the flow topology of Fig.1a (no hinge points) for the first two curves and the two-hinge-points regime for the third curve. All three curves have two blips (maxima) which indicate that in the near-blip zone of the exterior plane the intensity of conduction into the slab is even higher than in the case of no thermal insulation, i.e. near the edges E_1 and E_2 in Fig.1a the barrier "sucks" energy.
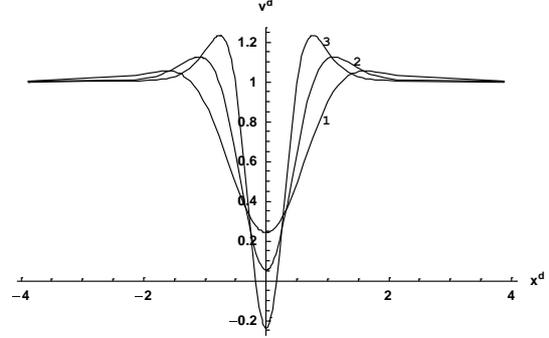

Fig.5. Vertical component of thermal gradient v^d as a function of x^d along AOD for r=0.5 and a^d=1, 2 and 4 (curves 1-3, correspondingly).

Without any series expansions we can bluntly use eqns. (6) and (9) in the following form:

$$w^d = iz^d - 1 - \frac{ir}{\pi}\int_{-1}^{1}\frac{F(\tau)\,d\tau}{\tau - \left(\dfrac{\exp[-\pi z^d]-1}{\exp[-\pi z^d]+1}\right)} \quad (17)$$

where dimensionless variables are introduced as $w^d = w/(k(T_0 - T_c)), \quad z^d = z/b$.

By the help of the routines *Re* and *Im* [9] we separated the real and imaginary parts in eqn.(17). Then we used the *ContourPlot* routine [9] to plot the flow nets. Fig.6 shows the flow net for F=exp[-$a^d(x^d)^2$] with r=0.9, and a^d=15 (two hinge points regime of Fig.3a). In Fig.6, in order to avoid cluttering, only three equipotential contours are presented: ϕ^d=-0.1 (curve 1, single branch, see the Riemann surface in Fig.3b), ϕ^d=-0.3 (two branches, labeled 2) and ϕ^d=-0.4 (two branches, labeled 3). For the sake of comparisons we also plotted the equipotentials according to the mentioned solution [3], denoted here as (CJ-2.19), which in our notations and dimensionless variables reads:

$$\phi^d(x^d, y^d) = \frac{1}{2}\sin\pi y^d \int_{-\infty}^{\infty}\frac{1 - r\exp[-a^d\tau^2]}{\cosh\pi(1-y^d) + \cosh\pi(x^d - \tau)}d\tau$$

(CJ-2.19)

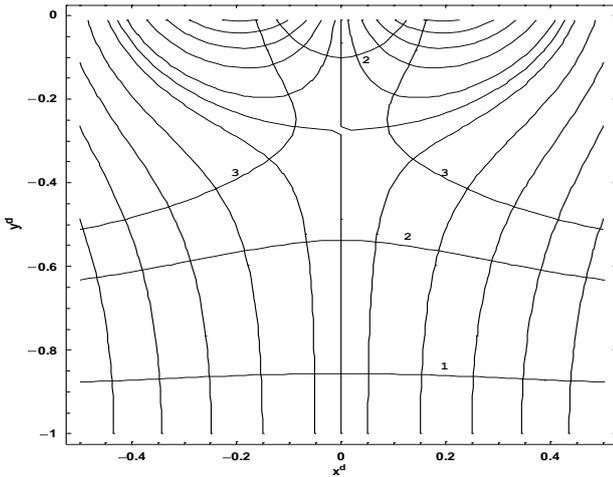Our eqn.(17) and eqn. (CJ-2.19) give identical contours.

Fig.6. Flow net (isotherms and heat lines) for $F=\exp[-a^d(x^d)^2]$, r=0.9, $a^d=15$

It is clear that S_3 in Fig.3a is indeed a saddle point, i.e. if we approach this point from the left and right, then temperature decreases towards this point, but if we move from S_3 upward and downward, then temperature decreases[1]. S_3 (in Fig.6 corresponds to the contour-plotting lacuna) is a genuine critical point because the thermal gradient there is zero while H_1 and H_2 are not really critical points (only v there vanishes but the horizontal component u of $\vec{J}$ does not). *Mathematica* contour-plotting computations confirmed what we conceptualized as flow topologies in Figs.1a, 2a, 3a.

3. Conclusions

Our mathematical model and the final solution, eqn.(17), gives temperature and heat flux field in the slab as an output of the *ContourPlot* routine of a standard computer algebra package (*Mathematica*). The solution is simple, versatile and provides analytical expressions for isotherms, heat lines, and thermal gradient (magnitudes and directions). Our solution gives the same results as the known solution from [3] (obtained by a different method and not analyzed by them). The flow topology in Figs.1-3 is indeed counterintuitive and, to the best of our knowledge, has never been reported before. Our mathematical approach to solve the corresponding boundary-value problem of heat conduction can be easily extended to more complex geometries of conducting elements than in the presented case (strip), e.g. a rectangle or other polygons can be studied (this would require a more general Schwartz-Christoffel mapping than eqn.(6)).

4. References
[1] Yu.V.Obnosov, R.G.Kasimova, A.Al-Maktoumi, A.R.Kacimov. Can heterogeneity of the near-wellbore rock cause extrema of the Darcian fluid inflow rate from the formation (the Polubarinova-Kochina problem revisited)? *Computers & Geosciences*, 36, 1252–1260. 2010. doi:10.1016/j.cageo.2010.01.014.
[2] Yu.V.Obnosov, R.G. Kasimova, A.R.Kacimov. A well in a 'target' stratum of a two-layered formation: the Muskat–Riesenkampf solution revisited. *Transport in Porous Media,* 2011, DOI 10.1007/s11242-010-9693-6
[3] H.S.Carslaw, J.C.Jaeger, *Conduction of Heat in Solids.* 2nd edition. Clarenden Press, Oxford, 1959.
[4] F.D.Gakhov, *Boundary Value Problems*, Pergamon Press, New York, 1966.
[5] P.Ya.Polubarinova-Kochina, *Theory of Groundwater Movement.* Princeton Univ. Press, Pinston, 1962.
[6] D.J. Sailor, D.Hutchinson, L.Bokovoy, Thermal property measurements for ecoroof soils common in the western U.S. *Energy and Buildings*, 40, 1246–1251, 2008.
[7] A.Bejan, *Convection Heat Transfer.* 3rd edition. Wiley, N.Y, 2004.
[8] J. A. Kolodziej, T.Strek. Analytical approximations of the shape factors for conductive heat flow in circular and regular polygonal cross-sections. *International Journal of Heat and Mass Transfer,* 44(5), 999-1012, 2001.
[9] S.Wolfram. *Mathematica. A System for Doing Mathematics by Computer.* Addison-Wesley, Redwood City, 1991.

---

[1] We recall that the maximum principle (valid for any elliptic equation and the Laplace equation used in this paper, in particular) prohibits global maxima and minima of temperature inside G_z.